Proceedings of ASME 2011 5th International Conference on Energy Sustainability & 9th Fuel Cell Science, Engineering and Technology Conference
ESFuelCell2011
August 7-10, 2011, Washington, DC, USA

ESFuelCell2011-54245

MODELING OF A PARABOLIC TROUGH SOLAR FIELD FOR ACCEPTANCE TESTING: A CASE STUDY

Michael J. Wagner
National Renewable Energy Laboratory
Golden, Colorado 80401
Email: michael.wagner@nrel.gov

Mark S. Mehos
National Renewable Energy Laboratory
Golden, Colorado 80401

David W. Kearney
Kearney & Associates
Vashon, Washington 98070

Andrew C. McMahan
SkyFuel
Arvada, Colorado 80007

ABSTRACT

As deployment of parabolic trough concentrating solar power (CSP) systems ramps up, the need for reliable and robust performance acceptance test guidelines for the solar field is also amplified. Project owners and/or EPC contractors often require extensive solar field performance testing as part of the plant commissioning process in order to ensure that actual solar field performance satisfies both technical specifications and performance guaranties between the involved parties. Performance test code work is currently underway at the National Renewable Energy Laboratory (NREL) in collaboration with the SolarPACES Task-I activity, and within the ASME PTC-52 committee.

One important aspect of acceptance testing is the selection of a robust technology performance model. NREL[1] has developed a detailed parabolic trough performance model [1] within the SAM software tool [2]. This model is capable of predicting solar field, sub-system, and component performance. It has further been modified for this work to support calculation at sub-hourly time steps.

This paper presents the methodology and results of a case study comparing actual performance data for a parabolic trough solar field to the predicted results using the modified SAM trough model. Due to data limitations, the methodology is applied to a single collector loop, though it applies to larger subfields and entire solar fields. Special consideration is provided for the model formulation, improvements to the model formulation based on comparison with the collected data, and uncertainty associated with the measured data. Additionally, this paper identifies modeling considerations that are of particular importance in the solar field acceptance testing process and uses the model to provide preliminary recommendations regarding acceptable steady-state testing conditions at the single-loop level.

NOMENCLATURE

ANI Aperture-normal insolation
ASME American Society of Mechanical Engineers
CSP Concentrating Solar Power
DNI Direct-normal insolation
DOE Department of Energy (US)

[1]The Alliance for Sustainable Energy, LLC (Alliance), is the manager and operator of the National Renewable Energy Laboratory (NREL). Employees of the Alliance, under Contract No. DE-AC36-08GO28308 with the U.S. Dept. of Energy, have authored this work. The United States Government retains and the publisher, by accepting the article for publication, acknowledges that the United States Government retains a non-exclusive, paid-up, irrevocable, worldwide license to publish or reproduce the published form of this work, or allow others to do so, for United States Government purposes.

EPC Engineering, Procurement, and Construction
HTF Heat transfer fluid
IAM Incidence angle modifier
NREL National Renewable Energy Laboratory
PTC Performance Test Code
PTM Physical Trough model
SAM System Advisor Model
SCA Solar Collector Assembly
SEGS Solar Electric Generation System
θ Theta; solar irradiation incidence angle

INTRODUCTION

The number of CSP plants under development or under construction has significantly increased in recent years. The need for standardized acceptance testing procedures is amplified as these plants approach the final stages of construction. Both NREL, in conjunction with Kearney & Associates, and the ASME PTC-52 working group are pursuing acceptance test standards for parabolic trough systems. NREL's expedited effort has produced an interim acceptance test guideline [3]. This paper compares performance data obtained from SkyFuel's test loop at the SEGS II facility in Daggett, CA, to performance predicted by the SAM Physical Trough Model (PTM) [1].

The trough Performance Test Code (PTC) provides a methodology for comparing the measured performance of a solar field to its expected performance. For complex CSP systems, determining the expected solar field performance is not a trivial exercise. CSP performance is subject to a number of uncontrollable effects. These include solar position, level of direct-normal irradiation (DNI), wind velocity, mirror soiling, and ambient temperature. While the effect of some variables - like DNI - is unquestionably more prominent than others, each significant effect must be quantified in order to obtain a sufficiently precise prediction of solar field performance. PTC tests for non-CSP processes often make use of correction curves to account for off-design operation. However, because of the complex and variable nature of CSP systems, a detailed performance model fills this role during the acceptance test process.

The acceptance test focuses on providing a statistically valid methodology for deciding whether a system's performance achieves its objective. Because no measurement technique can perfectly determine the quantity it measures (e.g. every measurement device has inherent uncertainty associated with the value that it reports), the acceptance test's goal is to determine whether the plant performance meets or exceeds the target, given a particular uncertainty and required confidence level. The performance metric will depend on the requirements of the project stakeholders; likely options include thermal efficiency and delivered thermal power. The measured values are compared to the target values provided by the detailed performance model and theoretically can be applied under any operating condition that both the performance model and the solar field can accommodate. Often, the goal of the performance test is not limited to thermal performance but also seeks to demonstrate the capability of the solar field to produce thermal energy at a particular capacity. For this reason, the test is sometimes constrained to a certain range of weather, solar resource conditions, and sun positions.

The capacity-based performance test measures the rate of energy delivery (power), instantaneous thermal efficiency, or some other metric that demonstrates field performance over a relatively short time span. Unlike baseload fossil or nuclear power plants, CSP systems are subject to a wide range of variability in energy input - in this case, the solar resource. In the course of operation, the plant will start up and shut down daily and operate under transient loads. The behavior of the plant during these phases of operation differs substantially from the clear sky "steady state" performance test. Stakeholders may be interested in demonstrating plant production over a longer period of time that includes these transients. The acceptance test procedure in [3] also provides recommendations for a multi-day production-based acceptance test. In either the production or capacity performance tests, an accurate and descriptive transient performance model is required. The following discussion provides additional details relating to the performance model used in this study, the acceptance testing procedure, and the results of the model-to-data comparison.

THE DETAILED PERFORMANCE MODEL

The detailed performance model provides an essential function in the acceptance testing process. Because the solar irradiation, wind velocity, sun position, etc., are rarely (if ever) simultaneously at their design-point values, the performance model serves as a robust performance correction device. The acceptance test performance model will typically be supplied by the project developer, technology provider, or EPC contractor who is knowledgeable of proprietary subsystem and component description parameters. This arrangement ensures that the model is sufficiently accurate and has been validated with respect to the constructed plant. Realistically, the performance model will be the same one used to produce the proforma estimates and will also be agreed between parties to monitor the warranty performance.

In this paper, the PTM is employed as the performance model. SAM uses user-input, representative default values, and approximations to predict system performance for a wide range of plant configurations. The PTM is capable of modeling a variety of plant configurations, including those with thermal storage, auxiliary fossil-fired backups, different field layouts, and different receiver/collector geometries. The analysis presented in this paper depends on the capabilities of the PTM, so the following discussion presents several important modeling considerations. Since the modeling requirements of an acceptance test

are somewhat different than for the typical annual simulation, several modifications to the PTM were required.

Sub-hourly time steps

The most commonly available weather data is reported on an hourly basis, but acceptance testing requires simulation on a much shorter time step. The PTM formulation was modified to accept simulation time steps between 1 second and 1 hour, corresponding to the frequency of data readings. The analysis presented in this paper uses 5-second data recorded at the acceptance test site.

Partial plant analysis

While the power generation cycle, thermal storage system, and balance-of-plant impact the performance of the solar field in their operation, the purpose of this acceptance test is to quantify the performance of the solar field. Therefore, the model boundary conditions must match the test boundary conditions.

During a typical "whole system" performance simulation, the HTF mass flow rate through the field is calculated depending on the desired field outlet temperature and the return HTF temperature from the power block. Thus, the solar field HTF inlet temperature, outlet temperature, and mass flow rate are all defined based on available solar resource and power block performance. During acceptance testing, the model is required to match conditions at the boundary of the test, so HTF conditions must be specified for every time step along with weather data.

The PTM was modified to allow specification of the HTF inlet temperature and either the instantaneous HTF mass flow rate or the desired HTF outlet temperature. With two of three required data values provided, the model calculates the third and considers the deviation between the calculated value and the observed/measured data value as the error. The energy balance is shown in Eq.(1) in terms of inlet/outlet enthalpy conditions, where enthalpy h is described by the product of specific heat and temperature ($c_p(T) \cdot T$). The specific heat is calculated as the integral-average with respect to temperature of specific heat values over the span of the modeled section of the solar field.

$$\begin{aligned} \dot{q} &= \dot{m}_{htf}\left(h_{sf,out} - h_{sf,in}\right) \\ &= \dot{m}_{htf}\, c_{p,htf}\, \left(T_{sf,out} - T_{sf,in}\right) \end{aligned} \tag{1}$$

In Eq.(1), the thermal energy absorption term $\dot{q}$ is modeled to be equal to the total incident radiation scaled by the optical efficiency, less any thermal losses. This is illustrated in Eq.(2).

$$\dot{q} = I_{bn}\, A_{aperture}\, \eta_{optical}(\theta)\, \cos(\theta) - \dot{q}_{loss,thermal} \tag{2}$$

Here, I_{bn} is the direct-normal irradiation in units of $\frac{W}{m^2}$, $A_{aperture}$ is the active mirror aperture area within the test boundary, $\eta_{optical}$ is the optical efficiency including incidence angle modifier (IAM) effects, $\cos(\theta)$ is the irradiation incidence angle adjustment factor, and $\dot{q}_{loss,thermal}$ is the total thermal loss from the test boundary.

It is important to distinguish between the modeled quantities and the measured (or calculated) quantities. The absorbed thermal energy in Eq.'s(1, 2) is a modeled quantity that is used to predict the HTF outlet temperature[2] given certain conditions for ANI, wind speed, etc. The absorbed thermal energy predicted by the performance model is juxtaposed with the measured-data calculations, where $\dot{q}$ is calculated based on direct measurement of inlet/outlet temperature and flow rate.

For the PTM, the inlet temperature constraint can be applied either at the power block heat exchanger outlet (thus including the thermal inertia and thermal losses of header piping), or it can be applied directly at the inlet of a single loop. The model provides calculated data for both the outlet temperature of a single loop and the return HTF temperature at the power block heat exchanger inlet. In either situation, it is imperative that the model accommodate the boundary conditions that are used during data collection.

Depending on the purpose of the acceptance test, the test boundaries may either be set immediately surrounding a single loop or around the entire solar field, as shown in Figure 1. Generally, the solar field acceptance test will maintain the test boundaries around the entire solar field so as to fully characterize the ability of the solar field to supply thermal energy to the power generation equipment. However, the nature of the data provided for this analysis relegated the boundary condition to the immediate inlet and outlet of a single loop.

Piping system geometry

For any acceptance test model comparison, it's important to match the model geometry to the actual plant geometry as closely as possible. Thermal losses, thermal inertia, and head loss across the solar field all contribute to solar field performance and all are sensitive to the field geometry. Since the PTM is a generalized model, several assumptions are used to provide both detail and flexibility in the field piping layout.

Field header layout First, the solar field is assumed to be divided into symmetrical subfields with the power block island geometrically in the center of all subsections. For a field with two subsections, each section to the west and east of the power block are mirror images; each receive the same HTF mass flow rate and are assumed to perform identically. For a field with four subsections, the power block lies in the center area between the northern and southern subfield groups. Again, HTF mass

[2] or the HTF mass flow rate, if both inlet and outlet temperatures are selected as constraints

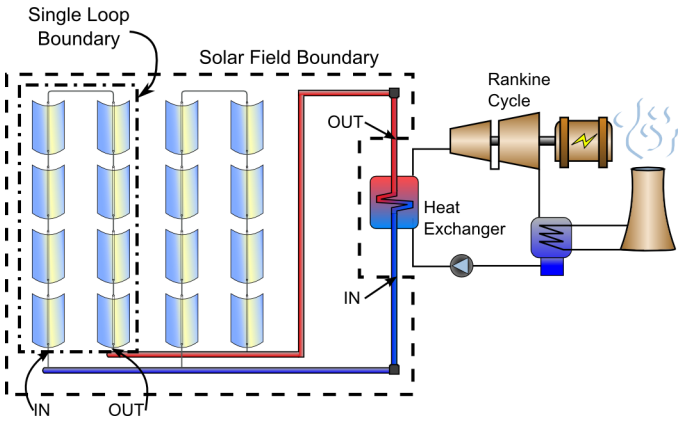

FIGURE 1. Possible boundary conditions for the solar field acceptance test. One boundary condition surrounds the entire solar field, excluding the power cycle heat exchanger; the other surrounds a single loop. The single-loop boundary is used in this analysis.

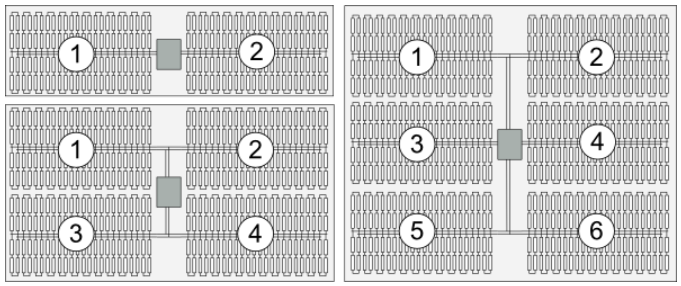

FIGURE 2. Aerial view of three possible solar field piping configurations, including a 2-subsection system (top left), a 4-subsection system (bottom left), and a 6-subsection system (right). The power cycle is shown as the dark section in the center of each field.

flow to the northern and southern groups is equal, and flow splits to the east and west subsections equally. Figure 2 illustrates plant configurations for 2, 4, and 6 subfields. The number of subfields is constrained to be divisible by 2.

The simulation results are dependent on the field piping layout since the thermal inertia associated with header piping corresponds to the number of loops per subfield and the distance that HTF must travel along the runner piping to reach the subfields. Since the analysis in this study considers a boundary condition around a single loop as shown in Figure 1, the field layout is not significant. However, if one were to select the solar field boundary delineated in Figure 1, the field layout would be a significant factor in understanding the acceptance test results.

Pipe sizing Cost-effective piping system design makes use of commonly available piping schedules for the sizing of header and subfield header piping. The PTM sizes the header and subfield header piping to maintain the HTF velocity *under design conditions* to be within the range specified by the user. The model chooses the smallest diameter piping from a piping schedule that both maintains material hoop stress constraints and maximum velocity constraints at design. By capturing these effects, the PTM models behavior that more closely approaches real CSP plants. The piping schedule and hoop stress constraints were adapted from [4].

Capturing transient effects

Capacity-based acceptance tests that measure system performance over a short period of time generally require steady-state conditions for the duration of the test. The term “steady-state”, strictly defined, requires that the solar field system demonstrate no change in inlet/outlet temperature and mass flow rate, and be subject to constant weather conditions like ANI, ambient temperature, wind speed, etc. Observations show that solar field systems are rarely (possibly never) in a true steady state; dynamic or transient behavior is always present to some degree.

Consequently, the steady-state constraint must be relaxed to accommodate small variations in system and weather conditions. Since the acceptance test relies on comparing observed performance data to modeled performance, the size of the allowable deviation from steady-state is a question of the required uncertainty of the measured results and the quality of the performance model. A model that fully captures transient behavior will maintain affinity with observed data more closely than a model that captures transient effects poorly or simplistically.

The PTM has incorporated major transient effects and adjustment factors in the performance equation formulations to better capture actual plant behavior. The PTM treats the solar field as a series of distinct nodes with mass, volume, temperature, and other attributes according to the position within the field and the components that the node represents. Each node is assumed to be fully mixed with a temperature gradient across the node. For example, each header is a single node; the mass, density, volume, and other properties of that node are calculated to represent the entire header, and the header node also has a temperature gradient applied from the inlet to the outlet of the header. Likewise, each SCA in the loop is a unique node with a temperature gradient according to thermal performance. This is illustrated for a single loop (excluding headers) in Figure 3.

The mathematical formulation to determine the outlet temperature of each node considering some timestep Δt includes the effect of changing inlet mass flow rate, temperature, absorbed thermal energy, thermal losses, and the thermal mass of the node. The thermal mass includes calculated HTF volume and a factor mc_{bal} that accounts for piping and insulation mass (if applicable). Eq.(3) shows the general formulation for non-active piping (headers and subfield header piping), and Eq.(4) shows the same

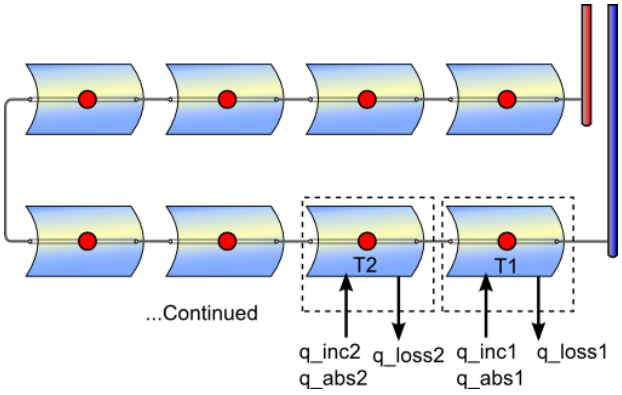

FIGURE 3. The nodal structure of a loop in the solar field. The PTM uses a nodal calculation approach to model solar field performance.

formulation for active receiver piping[3].

$$T_{hdr} = \left(T_{hdr,0} - T_{htf,in}\right) \cdot \exp\left[-\frac{\dot{m}_{in}}{\overline{v}\,\rho + \frac{mc_{bal,hdr}}{c_{p,htf}}} \cdot \Delta t\right] + T_{htf,in} \quad (3)$$

$$T_{SCA} = \left(\overline{T}_{SCA,0} - T_{htf,in} - \frac{\dot{q}_{abs}}{2 \cdot \dot{m}_{in}\, c_{p,htf}}\right) \cdot 2\,\exp\left[-\frac{2\,\dot{m}_{in}}{\overline{v}_{SCA}\,\rho_{SCA} + L_{SCA}\frac{mc_{bal,SCA}}{c_{p,htf}}} \cdot \Delta t\right] + \frac{\dot{q}_{abs}}{\dot{m}_{in}\, c_{p,htf}} + T_{htf,in} \quad (4)$$

where T_{hdr} is the outlet header temperature, $T_{hdr,0}$ is the temperature of the same node from the previous time step, $\overline{v}$, ρ, and $c_{p,htf}$ are the temperature-dependent nodal volume, density, and specific heat in Eq.(3). In Eq.(4), T_{SCA} is the SCA outlet temperature, $\overline{T}_{SCA,0}$ is the average temperature of the same node from the previous time step, L_{SCA} is the length of the SCA, $\overline{v}_{SCA}$ is the HTF volume in the node, ρ_{SCA} is the HTF density, and $\dot{q}_{abs}$ is the absorbed thermal energy. For the current analysis, the mc_{bal} terms were calculated based on the detailed piping model in [4].

Model limitations Unlike a "plug flow" model that tracks the position of finite quantities of HTF passing through the solar field, the nodal model formulation in the PTM cannot include any strict time delay between a change in the solar field inlet boundary conditions. However, the nodal approach does produce the effect of a time delay since boundary condition changes are propagated from node to node with successively diminished effect, but the behavior differs slightly from an actual system. To predict the impact of the nodal model formulation compared to a more realistic system, we performed a simplified analysis contrasting the behavior of a plug flow model with an equivalent "fully mixed" nodal model. Both models considered the impact of a step-change in HTF temperature at the inlet of a long insulated steel pipe carrying Therminol-VP1^{TM}.

[3]The derivation of these equations is described in [5]

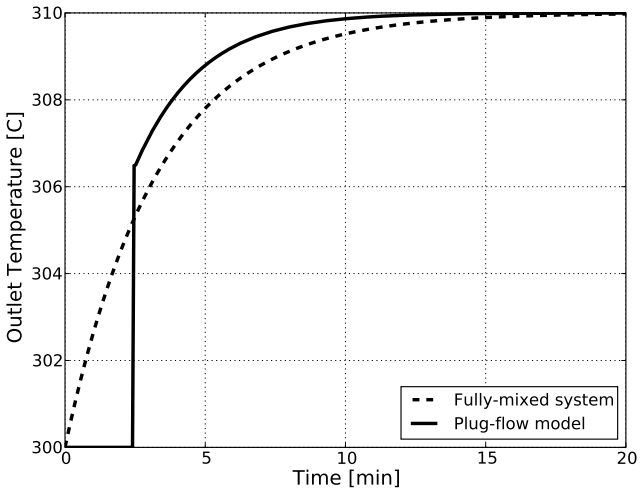

FIGURE 4. Response of a plug-flow type model and a nodal type model to a step-change in inlet temperature. The plug flow model behaves similarly to an actual piping system; however, the fully mixed model approximates the behavior reasonably well for longer time steps.

Figure 4 illustrates the results for the comparison between a nodal pipe model and a plug flow model. The plug flow model behaves more like a typical solar field in this situation; after a step change in the inlet HTF temperature, the outlet temperature does not respond for several minutes, then gradually approaches the inlet temperature as the piping and insulation warms. The fully mixed model outlet temperature responds immediately to a perturbation in the inlet temperature and continues to increase until coming to steady state at the inlet temperature value.

After examining Figure 4, several interesting conclusions become apparent. Specifically, (1) the nodal model approaches the behavior of a real system (represented by the plug flow model) at time steps that are 2-4 times longer than the HTF traversal time, (2) the nodal model is especially error-prone immediately after a step-change in the inlet boundary conditions, and (3) as a general rule, the nodal model takes 25-35% longer to observe a step-change effect as compared to a real plant. However, transient concerns are irrelevant so long as the acceptance test is conducted during sufficiently steady-state conditions.

In addition to limitations associated with the mathematical formulation, the accuracy of the model results are contin-

gent on the quality of the model inputs, optical efficiency terms, boundary conditions, and semi-empirical heat transfer correlations used in the model. Proper modeling technique also plays a role in producing accurate model output. Since acceptance testing calls for comparison of measured data to predicted model results as a basis for plant acceptance, test parties must carefully consider all aspects of the performance model before testing. While no model can predict performance of a complex system with perfect accuracy, the model *can* establish a required minimum performance level by using model inputs and performance characterization techniques that the technology provider is willing to contractually guarantee.

UNCERTAINTY ANALYSIS APPROACH

The trough performance acceptance test seeks to answer the question of whether various measured performance metrics compare favorably to guaranteed results. A meaningful answer to this question requires accurate data measurement tools; however, any real measurement system has both random and systematic (bias) errors associated with the reported values. The systematic error associated with a measurement of a single parameter can come from many sources including the calibration process, instrument systematic errors, transducer errors, and fixed errors of method. The test engineer should be diligent in identifying all of these sources of error, although it is often the case that one or several will dominate within a particular measurement parameter.

Both random and systematic error can be based on a manufacturer's specification. However, unlike systematic error, the random uncertainty for a given measurement can be reduced based on repeated measurements over the interval in which the system is considered to be at steady state (defined by a minimal change in the ANI plus HTF flow control over the test period such that the effects of thermal exchange between the HTF and solar field piping are negligible). For repeated measurements, the random standard uncertainty can be defined by:

$$s_{\overline{X}} = \frac{S_X}{\sqrt{N}} \tag{5}$$

where S_X is the standard deviation of a series of sample data and N is the number of data points collected over the test interval [3].

Often, the final goal of the acceptance test is to compare metrics like solar field thermal power output or thermal efficiency with analogous modeled metrics. These metrics can't be measured directly, but are amalgamations of several measured quantities. As described in [3], the final metrics are calculated using the average value of the measured data over the course of the acceptance test. Generically, each calculated result is a function of all of the i averaged values used to calculate it, as shown in Eq.(6).

$$R = f\left(\overline{X_1},\, \overline{X_2},\, ...,\, \overline{X_i}\right) \tag{6}$$

The resulting uncertainty u for calculated result R is determined by combining the systematic error b_R and random error S_R via root-sum-square.

$$u_R = \left[b_R^2 + S_R^2\right]^{1/2} \tag{7}$$

The systematic and random error terms are calculated by summation of the I equation terms as shown in Eq.'s(8, 9).

$$b_R = \left[\sum_{i=1}^{I} \left(\frac{\partial R}{\partial \overline{X_i}}\, b_{\overline{X_i}}\right)^2\right]^{1/2} \tag{8}$$

$$S_R = \left[\sum_{i=1}^{I} \left(\frac{\partial R}{\partial \overline{X_i}}\, S_{\overline{X_i}}\right)^2\right]^{1/2} \tag{9}$$

The partial derivative terms symbolically represent the manner in which the response R varies with the changing independent variable. For example, the response of thermal power to mass flow rate given Eq.(1) is:

$$\frac{\partial \dot{q}}{\partial \dot{m}_{htf}} = c_{p,htf}\, \left(T_{sf,out} - T_{sf,in}\right) \tag{10}$$

Extending the principle shown in Eq.(10) to the entire systematic uncertainty calculation for solar field thermal power yields Eq.(11).

$$\begin{aligned} b_R^2 = {} & \left(\frac{\partial R}{\partial \dot{m}} b_{\dot{m}}\right)^2 + \left(\frac{\partial R}{\partial c_p} b_{c_p}\right)^2 + \\ & \left(\frac{\partial R}{\partial T_{in}} b_{T_{in}}\right)^2 + \left(\frac{\partial R}{\partial T_{out}} b_{T_{out}}\right)^2 \end{aligned} \tag{11}$$

$$\begin{aligned} = {} & \left(c_p\, (T_{out} - T_{in})\right)^2 b_{\dot{m}}^2 + \left(\dot{m}\, (T_{out} - T_{in})\right)^2 b_{c_p}^2 + \\ & \left(\dot{m}\, c_p\right)^2 b_{T_{out}}^2 + \left(\dot{m}\, c_p\right)^2 b_{T_{in}}^2 \end{aligned} \tag{12}$$

The random error term S_R can be calculated likewise. The methodology in this example applies to any performance metric, so long as proper care is taken to quantify the error for each term in the calculation. Note that the uncertainty treatment in this example ignores the dependence of the fluid properties on

temperature; an expanded uncertainty analysis can be included to account for these effects. The final uncertainty term u_R is the standard uncertainty, and this can be used to determine confidence intervals (CI). Acceptance tests commonly use a 95% CI.

$$U_{R,95} = 2\,u_R \tag{13}$$

SYSTEM DESCRIPTION

The methodology presented above was applied to a data set provided by SkyFuel from their test loop at the SEGS II facility in Daggett, CA, for a clear July day. The SkyFuel test loop uses a set of collectors with an aperture width of 6 m and length of 13.7 m. Each SCA includes 8 mirror modules for a total of 656 m^2 net aperture area per SCA. The collectors are laminated with ReflecTech® Mirror Film in place of traditional silvered glass. The receiver used on each collector is the Schott PTR®-80. For more information on the system configuration, refer to [6].

Instrumentation for data collection is provided at the immediate inlet and outlet of the single test loop as shown by the single loop boundary in Figure 1. Since the single test loop is integrated into the larger SEGS II plant, the loop inlet conditions and mass flow are controlled externally and are not customized for the SkyFuel test loop configuration. Weather data are collected using on-site instrumentation.

RESULTS

Figure 5 shows both the modeled and observed thermal power output over the course of the day. The test period that was selected for this analysis falls between 13:40 (Pacific Standard Time) and 13:55. The data readings were 5 seconds apart for a total of 180 readings over the 15-minute test duration. Figure 5 also shows the acceptance test window.

This time period was selected since it corresponds to a relatively steady solar resource level. The test duration of 15 minutes was selected based on the data reading time step of 5 seconds and the number of test readings that allow a statement concerning system thermal output with a statistical confidence of 95%. As discussed below, shifting the selected time period to earlier in the afternoon would not change the result of the test in a statistically significant way, even though the model slightly over-predicts system performance during this time.

The uncertainty for measured data is provided in Table 1. This result provides the uncertainty contributions of the various measured data parameters over the course of the acceptance test time period. The reported uncertainty for specific heat is the largest of the various measurements because of the difficulty of measuring this physical quantity at high temperatures. This is an area of active exploration and future measurement techniques should reduce this uncertainty. The uncertainty contributions reported in Table 1 are combined to determine the total solar field

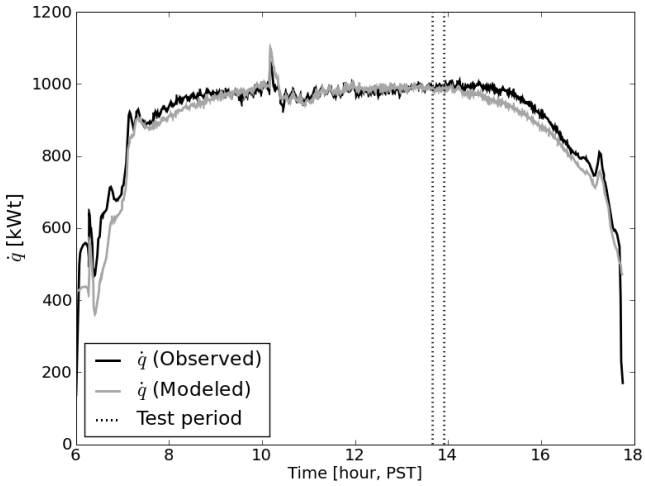

FIGURE 5. Comparison of observed thermal output and modeled thermal output over the course of the test day. The acceptance test window is also shown.

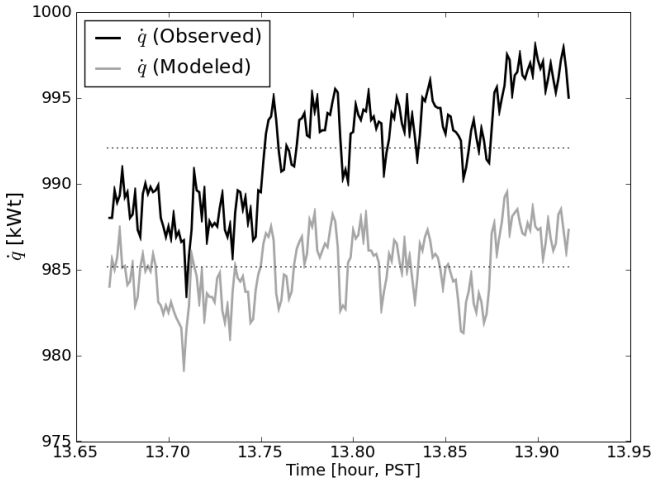

FIGURE 6. Comparison of observed thermal output and modeled thermal output over the course of the acceptance test. The average values are also indicated.

thermal output uncertainty[4]. The results of this analysis are provided in Table 2. The parties to the acceptance test should also agree on representative uncertainty values for model inputs like ANI and reflectance and factor these into the analysis.

In order to establish whether the system has passed the acceptance test, a comparison must be made between the observed data (along with its uncertainty distribution) and the modeled

[4]These tables are provided in the standard ASME PTC format for reporting uncertainty. For more information, refer to ASME PTC 19 or PTC 4 [7].

TABLE 1. Results of statistical analysis considering the calculated loop thermal output power as a function of the measured collector loop data.

Parameter Information (in parameter units)										Uncertainty contribution of parameters to the result (in units squared)	
Column name reference (see below)							*A*	*B*	*C*	*D*	*E*
Symbol	Description	Units	Relative unc.	Nominal unc.	Standard dev.	N_i	$b_{\overline{x_i}}$	$s_{\overline{X_i}}$	$\frac{\partial R}{\partial \overline{X_i}}$	$\left(\frac{\partial R}{\partial \overline{X_i}} s_{X_i}\right)^2$	$\left(\frac{\partial R}{\partial \overline{X_i}} b_{X_i}\right)^2$
m	Mass flow rate	$\frac{kg}{s}$	1.00%	5.56	0.009	180	0.056	0.001	178.3	98	0
c_p	HTF spec. heat	$\frac{kJ}{kg-K}$	1.25%	2.19	0.000	35	0.027	0.000	453.4	154	0
T_{out}	Hot HTF temp	$^\circ C$	0.32%	308.5	0.173	180	1.0	0.013	12.2	148	0
T_{in}	Cold HTF temp	$^\circ C$	0.44%	227.0	0.147	180	1.0	0.011	12.2	148	0

TABLE 2. Summary of the solar field power uncertainty calculation.

			Calculated Value ($\dot{q}$)	*A*	*B*	Combined standard unc.	Expanded result unc.	Expanded result unc.
Symbol	Description	Units	R	b_x	s_x	U_R	$U_{R,95}$	$U_{R,95}$ (%)
P	Solar field power	kJ/s	992	23	0	23	47	**4.7%**

Column definitions for Table 1 and Table 2

A Absolute systematic standard uncertainty

B Absolute random standard uncertainty

C Absolute sensitivity

D Absolute systematic standard uncertainty contribution

E Absolute random standard uncertainty contribution

data. In statistical terms, we seek to test the "null hypothesis": namely, that the observed thermal output does *not* exceed the modeled thermal output. Clearly, the point of an acceptance test is to demonstrate that the loop thermal output meets or exceeds a certain predicted output level, so if the null hypothesis is proved false[5], the test concludes that the system has passed the acceptance test.

Note from Table 2 that the mean observed thermal output value is 992 kWt with a 2σ uncertainty of 4.7% or 47 kWt at 95% confidence. Therefore, to prove the null hypothesis, the mean modeled thermal output value should exceed $992 + 47 = 1039 kWt$. In other words, a modeled thermal output greater than 1038 kWt would indicate with 95% confidence that the solar field is not performing at the guaranteed level predicted by the performance model. Figure 6 shows the observed and modeled thermal output along with the corresponding average values for the duration of the acceptance test.

The mean modeled thermal output value for this test period is 985 kWt - well below the 1039 kWt value that would prove the null hypothesis. Thus, the null hypothesis is disproved and the system has passed this acceptance test based on the thermal output criteria. Other test criteria such as thermal efficiency can be considered similarly, as discussed in [3].

Conclusions

This paper demonstrates the acceptance test process by comparing actual solar field data to SAM's detailed trough plant model. Since CSP systems are subject to widely varying boundary conditions, their expected performance is best characterized by a detailed performance model such as the PTM. The performance model is interwoven into the performance acceptance test

[5] Alternatively, consider that this test seeks to prove that the solar field doesn't underperform compared to the model. This statement is equivalent to proving the null hypothesis false.

process and should be acceptable to all parties involved.

The analysis presented in this paper shows that a carefully constructed performance model can accurately predict solar field performance on the single-loop level. However, test parties should understand the limitations of their selected performance model and quantify the potential limitations introduced by the model's formulation as demonstrated in Figure 4. Performing the acceptance test during steady-state conditions will minimize modeling anomalies. The best performance model will typically be the proprietary model provided by the solar field provider, though this does not exclude high-quality third-party models.

Given the relatively wide uncertainty band associated with measured data, some deviation in modeled results from observed or calculated results is expected. However, test parties should consistently seek to understand and minimize both systematic and random error in measurement devices and fluid properties. Since the recommended duration of a statistically valid acceptance test is relatively short (15 minutes at 5-second data readings), test parties may choose to conduct multiple acceptance tests throughout a single day or over multiple days. This both reduces the likelihood of a false result and demonstrates performance in varying weather conditions.

REFERENCES

[1] Wagner, M., Blair, N., and Dobos, A., 2010. "A detailed physical trough model for NREL's Solar Advisor Model". Proceedings of the 2010 SolarPACES International Symposium.

[2] Gilman, P., 2010. *Solar Advisor Model User Manual*, latest ed. National Renewable Energy Laboratory, Golden, Colorado. See also URL `www.nrel.gov/analysis/sam/publications`.

[3] Kearney, D., 2011. Utility-scale parabolic trough solar systems - performance acceptance test guidelines. Subcontract Report NREL/SR-5500-48895, Kearney & Associates, Vashon, Washington. Contract No. AXL-9-99218-01.

[4] Kelly, B., and Kearney, D., 2006. Parabolic trough solar system piping model: Final report. Tech. Rep. NREL/SR-550-40165, National Renewable Energy Laboratory, Golden, Colorado, USA.

[5] Wagner, M., 2010. "A detailed physical trough model for nrel's solar advisor model". Proceedings of the SolarPACES International Symposium, SolarPACES. NREL/CP-5500-49368.

[6] McMahan, A., White, D., Gee, R., and Viljoen, N., 2010. "Field performance validation of an advanced utility-scale parabolic trough concentrator". Proceedings of the SolarPACES International Symposium, SolarPACES. Publication pending.

[7] AMERICAN SOCIETY OF MECHANICAL ENGINEERS, 2005. *ASME Codes and Standards - Test Uncertainty*, ptc-19-1-2005 ed. New York, New York.